Journal of Chromatography A, 1218 (2011) 3973–3981

Contents lists available at ScienceDirect

Journal of Chromatography A

journal homepage: www.elsevier.com/locate/chroma

Reduced surface area chromatography for flow-through purification of viruses and virus like particles

Ganesh Iyer[a,*], Senthilkumar Ramaswamy[b], Damon Asher[a], Ushma Mehta[a], Anne Leahy[a], Franklin Chung[a], Kwok-Shun Cheng[a]

[a] EMD Millipore, 80 Ashby Road, Bedford, MA 01730, USA
[b] Lonza Biologics Tuas Pte. Ltd., 35 Tuas South Ave. 6, Singapore 637377, Singapore

ARTICLE INFO

Article history:
Received 2 March 2011
Received in revised form 26 April 2011
Accepted 28 April 2011
Available online 6 May 2011

Keywords:
Purification
Influenza
Virus
Nano-particle
Ion exchange
Chromatography

ABSTRACT

A method for flow-through purification of viruses and virus like nano-particles using a combination of binding and size-exclusion chromatography was developed. This technique relies on minimizing the external surface area per unit volume available for virus binding by increasing the mean diameter of the beads used in the column. At the same time the impurity binding capacity of the column is maximized by utilizing beads with multiple functionalities of the optimum size. Purification of different types of viruses and virus-like-particles could be achieved using this technique. Flow-through purification of influenza virus using this technique yielded virus recoveries greater than 70–80% coupled with impurity removal greater than 80%. Finally an approach to optimize and facilitate process development using this technology is presented. Since the impurity binding occurs via a non-specific mechanism and virus recovery is achieved through reduced surface area, the technique is not limited to specific types of viruses and offers the potential as a universal purification tool.

1. Introduction

Improving virus recovery, minimizing validation requirements and fast tracking purification are major downstream processing challenges in the vaccine industry. These challenges have gained significant importance in recent times due to pandemic outbreaks, vaccination on a large scale and newer upstream technologies to produce viruses. Current industry approaches to purify vaccines include gradient centrifugation, tangential flow filtration and bind/elute chromatography. Gradient centrifugation has traditionally been the workhorse of this industry and has come to be known as the most cumbersome and rate limiting unit-operation in vaccine production. Gradient centrifugation provides pure, concentrated product but suffers from drawbacks such as poor scalability, batch operation, low yields and loss of infectivity [1–3]. Although efforts have been made to make this process more continuous and improve product recoveries [4–8] the variability in yields for different viruses, high capital and operational costs and rigorous validation requirements associated with this process are good reasons to develop technologies to replace this unit operation.

Chromatography is an emerging alternative being considered for this application. Most known chromatography techniques for virus purification are based on a bind and elute mode of operation using anion exchange [9], affinity [10] or pseudo-affinity resins [11]. For anion exchange based purification the virus and impurities are bound to the media and then selectively eluted using a salt gradient. However, since the size of viruses is generally larger than the pores of commercially available resins they bind only to the external surface of the beads (Fig. 1) which results in poor virus capacity. Common approaches to improve capacities include use of smaller beads [12], beads with extenders [13], membranes [14] and emerging technologies such as monoliths [15,16]. All these approaches are geared towards increasing the available surface area for binding the virus. But they come with inherent drawbacks such as increased impurity binding to the media and larger pressure drops across the resin columns. Further the virus needs to be carefully eluted from the media using a salt gradient so as to ensure minimal contamination by co-eluting impurities such as host cell proteins (HCP) and host cell DNA (HC-DNA). This gradient fractionation leads to either poor yield or purity of product.

These drawbacks of bind and elute chromatography can be overcome if the media is able to selectively bind impurities while the virus passes through. Flow-through chromatography is commonly

* Corresponding author at: EMD Millipore, Purification Product Development, 80 Ashby Road, Bedford, MA 01730, USA. Tel.: +1 781 533 5624; fax: +1 781 533 8981.
E-mail addresses: ganesh.iyer@merckgroup.com (G. Iyer), senthil.ramaswamy@lonza.com (S. Ramaswamy), damon.asher@merckgroup.com (D. Asher), ushma.mehta@merckgroup.com (U. Mehta), anne.leahy@merckgroup.com (A. Leahy), ks.cheng@merckgroup.com (K.-S. Cheng).

0021-9673/$ – see front matter © 2011 Elsevier B.V. All rights reserved.
doi:10.1016/j.chroma.2011.04.086

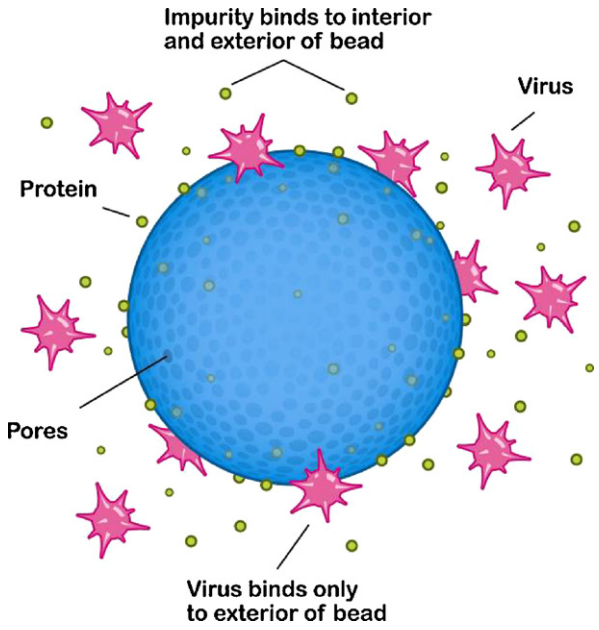

Fig. 1. Nature of virus versus protein binding to chromatography resins. Virus binding is limited only to the external surface of resins whereas proteins bind to both the external and internal surfaces of resins.

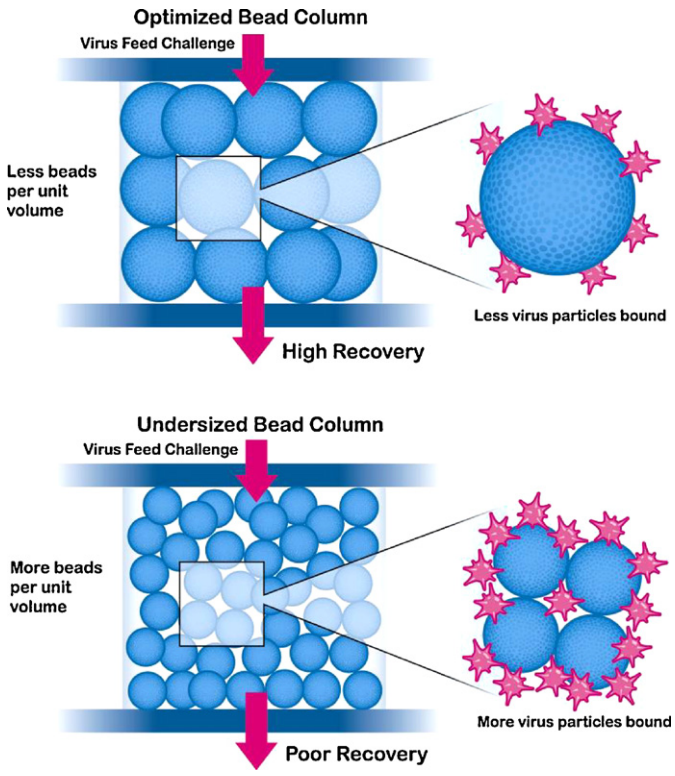

Fig. 2. Flow-through purification of viruses using columns with small and big beads.

used for trace impurity removal from monoclonal antibody feed streams [17,18]. It has several advantages over bind and elute mode of operation such as operational convenience, minimal use of buffers, continuous mode of operation, high productivity, high purity and high product recoveries. Using chromatography resins that bind to both the target molecule and impurity in a flow through mode would result in a significant loss of product. In the case of large biomolecules such as viruses, the binding is limited to the external surface area of the bead but is still significant. To achieve flow-through separation of large particles such as nano-particles and DNA which are similar in size to viruses researchers have proposed synthesizing charged beads with an inert surface layer [19] or coating charged beads with a neutral coating [20]. This would allow complete recovery of large particles due to exclusion by the smaller pores of the non-binding neutral surface layer while allowing diffusion of smaller impurities such as host cell protein into the internal charged surface of the bead. However, investigation of such beads in our laboratory through dynamic binding experiments (results not published) suggested that that neutral coatings as thin as 2 μm can cause considerable diffusional resistance for impurities to access the internal binding surface of the beads. This is partly because the initial concentration gradient across the inert boundary layer is shallow due to the non-binding surface. Hence this type of separation necessitates extremely large residence times or long columns lengths thereby limiting its practical application in a flow-through mode of operation. An alternate approach to minimize the loss of product due to binding to the external surface of the resins is by reducing the available surface area for binding. This can be accomplished by increasing the size of the beads used in a column which would in turn reduce the external surface area per unit volume. For example, as seen from the following equation:

$$\frac{n_1}{n_2} = \frac{A_1}{A_2} = \frac{D_2}{D_1}$$

where n_1 and n_2 are the number of virus particles bound to beads of two different sizes. A_1 and A_2 are the external surface area per unit volume due to beads of two different diameters D_1 and D_2.

Doubling the diameter of beads used in a column could lead to a drop in virus binding by 50%. Therefore, as seen in Fig. 2, as the size of the beads increases, the number of virus particles bound to the column decreases, thus resulting in increased recovery.

While the external surface area per unit volume decreases with increase in bead size the internal surface area available for impurity binding is not expected to decrease significantly as this is several orders of magnitude greater. Thus impurities such as host cell protein can be bound to the column in normal dynamic binding mode without any external diffusion limitations as in the case of coated beads. Larger beads could result in the impurities requiring additional time to penetrate into the beads and hence a nominal increase in the residence time in the column. However, good impurity removal along with improved virus recovery could be achieved by optimizing the bead size and processing time.

In this study the above proposed theory was verified using virus like nano-particles and live viruses. Flow-through purification of influenza virus from an impure feed was demonstrated. The effect of parameters such as bead size, bead functionality and feed throughput were evaluated. Finally a method to optimize such a purification was proposed. While this paper is geared towards virus purification this concept could be used for purifying any particle larger than the pore size of a bead.

2. Materials and methods

2.1. Materials

Chromatographic beads of various sizes and functionality were obtained from GE Healthcare. The beads used in the study included neutral beads of Sephraose FF (90 μm); anion exchange (AEX) beads of Q Sepharose HP (34 μm); Q Sepharose FF (90 μm) and Q Sepharose Big Beads (200 μm); cation exchange (CEX) beads of SP Sepharose FF (90 μm); SP Sepharose Big Beads (200 μm) and hydrophobic interaction (HIC) beads of Phenyl Sepharose FF (90 μm) and Phenyl Sepharose Big Beads (200 μm). Bovine serum albumin (BSA) was obtained from Sigma–Aldrich Corporation.

BSA-coated latex particles (100 nm) were obtained from Postnova analytics (Z-PS-POS-009-0,100). Buffers for chromatography experiments were prepared using DI water from a MilliQ® water purification system and molecular biology grade salts obtained from Fischer Scientific or Sigma–Aldrich. All buffers were filtered using a 0.2 μm Stericup® filters (EMD Millipore) prior to use.

2.2. Virus production and feed preparation

2.2.1. Bacteriophage ϕ6

Pure bacteriophage ϕ6 was first grown in *Pseudomonas pseudoalcaligenes* cells and purified using cesium gradient ultracentrifugation to obtain a highly concentrated stock solution. In brief, *P. pseudoalcaligenes* were first incubated in cell culture medium until it reached the appropriate cell density. Following this step, the cells were inoculated with a host culture of ϕ6 to achieve a MOI (multiplicity of infection) of 0.5 and incubated overnight. The cell debris was then pelleted and the virions eluted from the debris by ultracentrifugation at 12,000–16,000 × *g* using 40 mM Tris buffer with 150 mM NaCl and 10 mM MgCl. The virions were further purified and concentrated using cesium gradient and then dialyzed into Tris buffer to remove any cesium from the solution. The purified concentrated stock solution of ϕ6 with a final concentration of 0.5% BSA was aliquoted and stored at −80 °C before further use.

A feed solution for chromatography experiments was prepared by spiking the bacteriophage stock solution (stock titer of ~1.1×10^{12} pfu/ml) into about 600 ml of PBS to achieve a final ϕ6 concentration of about 10^8–10^9 pfu/ml. To determine if presence of proteins affected the virus recovery BSA was also added to the feed solution to achieve a final concentration of 0.18 mg/ml determined by UV spectroscopy.

2.2.2. Human influenza virus-type B

Approximately 200 ml of feed containing human influenza virus type B was grown using standard mammalian cell culture techniques in MDCK cells. Initially, eight T150 flasks were seeded with about 2.0×10^7 cells/flask in 10% FBS DMEM. After 24 h, the media in the flasks was changed to 1% FBS in DMEM and the cells were infected with influenza virus type B strain B/Lee/40 (ATCC # VR-1535) which was tissue culture adapted to growth in MDCK cells. The flasks were then incubated at 37 °C in 5% CO_2 for 5 days until complete CPE (cytopathic effect) was observed. The culture was subsequently centrifuged at 2500 RPM and the supernatant was filtered through a 0.45 μm membrane filter (Millipore Corporation) to remove cell debris and stored at 4 °C until further use. This neat clarified cell culture supernatant with an average virus titer of 64 HAU/ml was directly used as feed for chromatography experiments without any further processing.

2.2.3. Human influenza virus-type A

Feed containing human influenza virus type A was grown in MDCK cells in a manner similar to that discussed above. In brief, fifty T150 flasks were first seeded at 10% confluency of MDCK cells in 10% FBS DMEM. After 2–3 days, once the cells were 80–90% confluent, the media in the flasks was changed to DMEM without serum and the cells were infected with influenza virus type A/WS (H1N1 strain, ATCC # VR-1520) which was tissue culture adapted to growth in MDCK cells. The flasks were then incubated at 33 °C in 5% CO_2 for 3 days until complete CPE was observed. The supernatant was subsequently centrifuged at 2500 RPM, filtered through a 0.45 μm membrane filter to remove cell debris and stored at −80 °C until further use.

To prepare feed for the chromatography experiment the frozen virus stock in DMEM was first thawed at 4 °C overnight. The stock was then transferred into 50 mM Tris buffer at pH 8 or 50 mM sodium phosphate buffer at pH 7.2 using 10 KD Centricon (EMD Millipore) centrifugal membrane devices. This buffer exchanged stock solution was used as feed for flow-through experiments. The average titers of influenza virus, total protein and host cell DNA (HC-DNA) in the final feed were 3840 HAU/ml, 274 μg/ml and 3 μg/ml respectively.

2.3. Chromatography

A single type of chromatographic bead or a combination of beads were flow packed in Omnifit columns (DIBA Industries, diameter – 0.66 cm) to volumes of 0.5–2.4 ml, depending on the experiment. Before using the columns for flow-through experiments the columns were qualified by acetone pulse method to ensure that they had good HETP and an asymmetry between 1.1 and 1.7. Flow-through experiments were performed manually using positive displacement pumps (Mighty-Mini, Scientific Systems Inc. or Watson Marlow). The pump and tubing were first sanitized using 20% ethanol and then flushed with water and column equilibration buffer. The virus feed was subsequently passed through the column pre-equilibrated in equilibration buffer and fractions were collected downstream of the column into eppendorf® tubes. Preliminary experiments to determine virus recovery were performed in dynamic mode by flowing feed through the columns at a constant flow rate of 1 ml/min, where as later experiments to optimize impurity removal were performed at 5 min residence time per media type in the column. No significant change in virus recovery was observed due to changes in flow rates.

2.4. Analytical methods

2.4.1. Bacteriophage ϕ6 concentration

Concentration of bacteriophage ϕ6 was determined using a plaque assay [17]. In brief, the ϕ6 samples were serial diluted and the added to a suspension of *P. pseudoalcaligenes* bacterial cells. The dilution was then plated on solid growth medium and incubated at 25 °C for 24 h until it formed plaques. The number of plaques were manually read and used to back calculate the original concentration of ϕ6 in the samples.

2.4.2. Influenza virus concentration

Flu virus break-through and recovery was measured by hemagglutinin assay (HA) using standard protocol, described previously [21,22]. In brief, serial two fold dilutions of samples in PBS were incubated in chicken blood (Biomerieux) or rooster blood (Lampire biological products) for a period of 2 h at room temperature. The plates were visually read to determine the dilution at which the final agglutination was observed. This dilution was noted as the HA titer (HAU) per 50 μl of sample and was used to calculate the HAU/ml. Any variability in data due to change in blood type or quality was minimized by performing assays at a normalized hematocrit and further normalizing the data to a internal flu standard that was assayed along with the samples in every plate.

2.4.3. Total protein concentration

Total protein concentration which was representative of the host cell protein (HCP) content in the samples was determined by bicinchoninic acid (BCA) assay [23] using Pierce BCA assay kit (Thermo Scientific). Samples were incubated in BCA reagent at 60 °C for 30 min and read for change in absorbance at 562 nm using a plate reader from Beckmann Coulter or Tecan Systems. The protein concentration was determined against a calibration curve established using BSA as standard, over a range of 5–250 μg/ml.

2.4.4. DNA concentration

Host cell double stranded DNA (HC-DNA) concentration was measured by a florescent assay using Quant-iT™ Picogreen assay

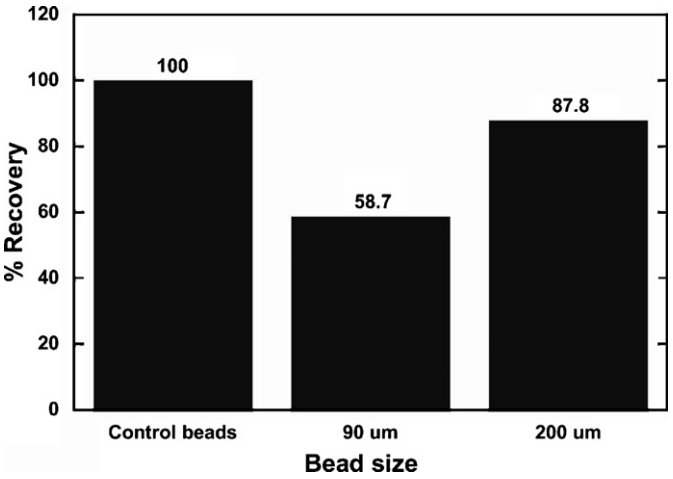

Fig. 3. Recovery of BSA coated latex particles form 90 μm and 200 μm Q Sepharose anion exchange beads and neutral 90 μm Sepharose FF control beads.

kit from Invitrogen [22]. HC-DNA containing samples were incubated with Picogreen reagent for 5 min at room temperature and then read using a plate reader at an excitation wavelength of 485 nm and emission wavelength of 565 nm. Concentration was determined against a calibration curve generated using Herring sperm DNA as a standard, over a range of 0.5 ng/ml to 2000 ng/ml.

3. Results and discussion

3.1. Static binding test of virus-like particles

Preliminary experiments to demonstrate proof of concept were done by studying static binding of BSA coated latex nano-particles to anion exchange (AEX) beads of two different sizes. BSA coated latex nano-particles make a good model for viruses since they have size and charge similar to common viruses such as influenza virus and herpes simplex virus [24–28]. AEX beads of 90 and 200 μm size and neutral beads of 90 μm size were separately gravity packed in columns to a volume of 5 ml and transferred into 7 ml lidded test tubes. The tube with neutral 90 μm beads was used as control to account for non-specific binding to the plastic tube and base matrix and dilution in the void volume of the beads. BSA coated latex particle solution (1.38 ml, 25 mg/ml, 1.4×10^{13} particles/ml) in PBS was added to each of the resin samples. The resin-particle mixture was rotated overnight, the beads were allowed to settle and absorbance of the particles in the supernatant was measured using UV spectroscopy at 280 nm. The concentration of the nano-particles in the supernatant was determined by UV absorbance using a calibration curve of different concentrations of the nano-particles. The percentage normalized recovery of BSA coated latex nano-particles at the end of the experiment was calculated using the following equations:

$$\%\,\text{normalized recovery} = \frac{(C_f/C_I)_{\text{bead}}}{(C_f/C_I)_{\text{control}}} \times 100$$

where C_I and C_f are the initial and final concentration (particles/ml) of the supernatant in the tubes. As seen in Fig. 3, the recovery of BSA coated nano-particles from 200 μm AEX beads was ~33% greater than 90 μm AEX beads verifying that increase in bead size can be used to reduce virus binding per unit volume of beads and thereby improve its recovery in a flow through mode.

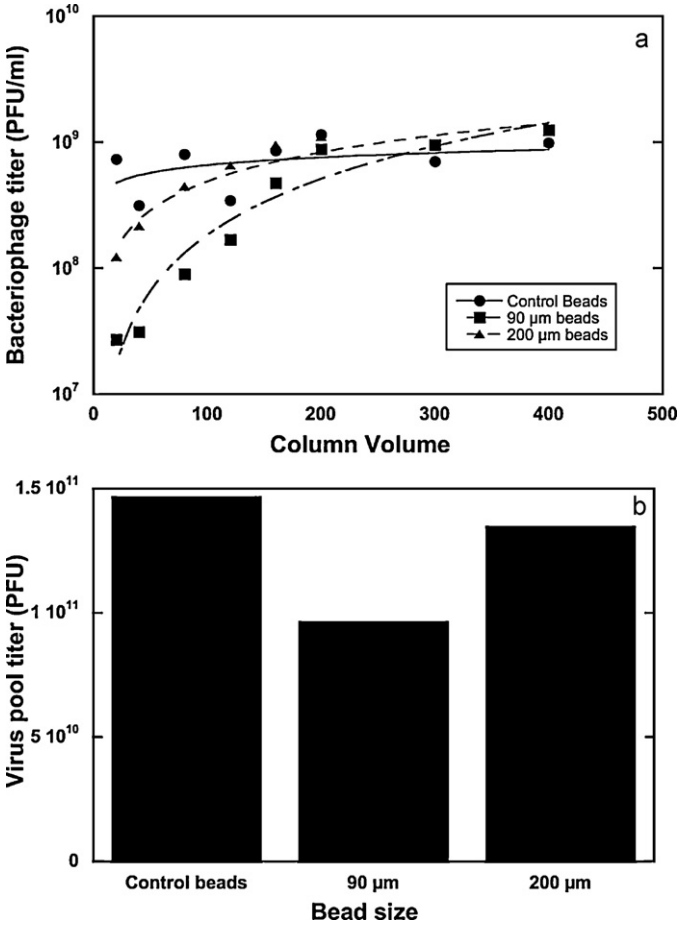

Fig. 4. Breakthrough and total recovery of bacteriophage ϕ6 from a solution of ϕ6 and BSA processed in a flow-through mode at a flow rate of 1 ml/min via 0.5 ml resin columns, each containing beads of a different size (a) nature of the virus breakthrough curve for [●] neutral 90 μm Sepharose FF, [■] 90 μm Sepharose Q FF and [▲] 200 μm Sepharose Q big bead columns. The lines are only a guide for the eye. (b) Total virus titer in the flow-though pool (measured in PFU) obtained from the 90 μm control Sepharose FF, 90 μm Sepharose Q FF and 200 μm Sepharose Q big bead columns.

3.2. Flow-through recovery of viruses

While the static binding studies described earlier provided proof of principle it was necessary to determine if this concept could be extended to recovery of live viruses in a dynamic mode. To evaluate this, the dynamic binding of two different viruses namely bacteriophage ϕ6 and influenza virus B/Lee/40 was studied in flow-through mode using AEX columns packed with beads of different sizes.

3.2.1. Bacteriophage ϕ6

The recovery of bacteriophage ϕ6 from a model feed stream prepared as described in Section 2.2.1 was evaluated as follows. Feed (200 ml, 400 column volumes (CV)) containing bacteriophage ϕ6 (5.9×10^8–1.1×10^9 pfu/ml) and BSA (0.18 mg/ml), was processed through 0.5 ml columns containing 90 μm or 200 μm anion exchange (AEX) beads and 90 μm neutral-control beads at a flow rate of 1 ml/min. The flow-through from the columns was collected in 10 ml fractions and the titer of ϕ6 in these fractions was plotted against the CV of feed processed to obtain the breakthrough curve for ϕ6. As seen from the breakthrough curves in Fig. 4a, the ϕ6 titer in the flow-through of the control beads instantly reached feed solution concentration suggesting negligible binding to these beads. The virus breakthrough curves for the 200 μm and 90 μm AEX beads reached the feed concentration only at ~150 CV and

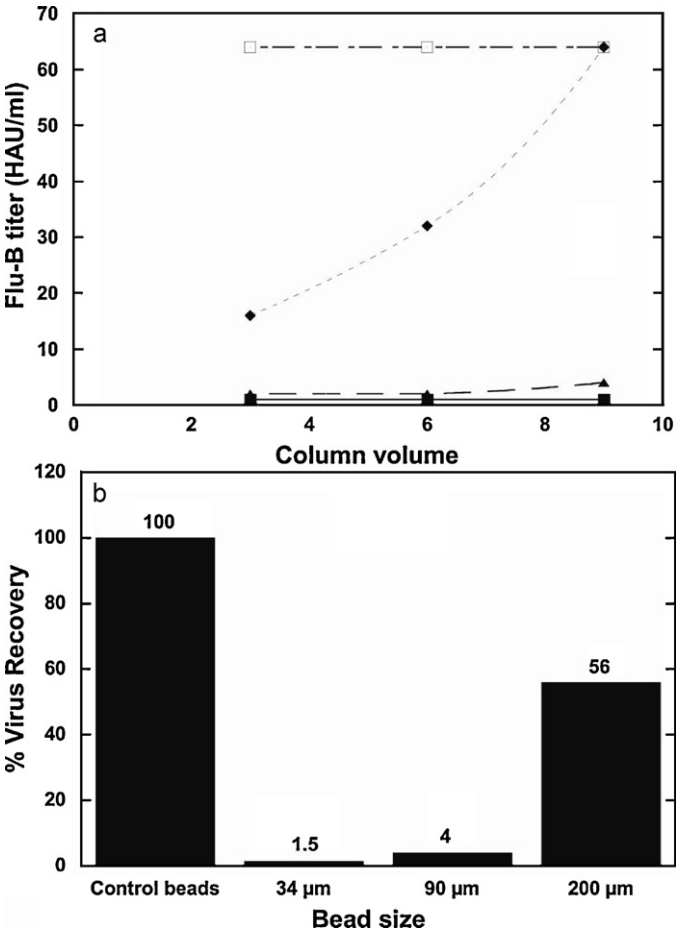

Fig. 5. Breakthrough and total recovery of influenza virus-type B (Flu-B) from a crude cell culture supernatant processed in a flow-through mode via 1 ml resin columns each containing beads of a different size at a flowrate of 1 ml/min (a) nature of the virus breakthrough curve for [□] neutral 90 μm Sepharose FF, [■] 34 μm Sepharose Q HP, [▲] 90 μm Sepharose Q FF and [♦] 200 μm Sepharose Q big bead columns. The lines are only a guide for the eye. (b) Total virus titer in the flow-though pool obtained from the 90 μm control Sepharose FF, Sepharose QFF, 34 um Q Sepharose HP, 90 μm Sepharose Q FF and 200 μm Sepharose Q big bead columns.

200 CV respectively. Also, the initial breakthrough titer at 20 CV for the 200 μm beads was ~1 log greater than the 90 μm beads. These observations suggest that AEX beads of both sizes bind the virus; however the 90 μm beads have higher virus capacity. The total virus recovery from each column was calculated from the area under the breakthrough curves and is shown in Fig. 4b. As expected the total virus recovery from the column containing 200 μm beads was one log greater than that of the 90 μm beads.

3.2.2. Human influenza virus-type B

The recovery of influenza virus strain B/Lee/40 from crude feed containing all cell culture impurities and additives such as HCP, HC-DNA, fetal bovine serum (FBS), non-essential amino acids was evaluated for 34 μm, 90 μm or 200 μm anion exchange (AEX) beads and 90 μm neutral-control beads. For this, 10 ml (10 CV) of crude feed was processed through 1 ml columns of each bead size at a flow rate of 1 ml/min. 1 ml aliquots of the flow through from each column was collected and assayed to determine the breakthrough curve for influenza virus strain B/Lee/40, shown in Fig. 5a. The area under the breakthrough curves was used to calculate the total recovery of virus from each column and is shown in Fig. 5b. For the volume of feed processed, the 34 μm bead column showed negligible breakthrough of virus, the 90 μm bead column showed initial breakthrough of virus at 10 CV, whereas the 200 μm beads showed instant breakthrough of virus and reached feed concentration by 10 CV giving an overall yield of 56%. Since the 200 μm AEX bead column had 2–6 times smaller surface area than the 34 μm and 90 μm AEX bead column it had very poor virus capacity which resulted in the much higher virus recoveries for the amount of feed processed through the columns. Processing larger amount of feed through the columns would improve the virus yields from all three AEX columns as observed for bacteriophage ϕ6; however, since the 200 μm bead column had an earlier virus breakthrough the overall yield from these beads will always be greater.

The results of the dynamic tests for both viruses are in accordance with the static binding studies. Both studies show the expected trend of increase in virus recovery with bead size due to decrease in surface area. It may be noted that the influenza virus strain B/Lee/40 breakthrough curve for the 200 μm AEX column reached the feed concentration much earlier than the bacteriophage ϕ6. This might be due to the large amount of impurities such as host cell protein, DNA and cell culture additives in the crude influenza feed that could compete for available sites on the surface of the bead causing earlier virus breakthrough. This effect may not be prominently seen for the 34 μm and 90 μm AEX bead columns over the amount of feed processed because of their considerably higher surface area that can dilute the effect. It can also be noted that the overall recovery of the influenza virus is lower than that for ϕ6. This could be an effect of the difference in sizes between the two viruses, limited amount of feed processed, or the lower influenza B virus titers used for this study.

The size of bacteriophage ϕ6 is ~78 nm [29] and that of influenza virus is ~80–120 nm [30]. This small difference in the size may not be significant enough to account for the lower influenza virus recovery observed in the study. Therefore, the most possible cause for the lower virus recovery should be the lower amount of feed processed. The effect of throughput has been further elaborated upon in Section 3.4. Based on the above studies it may be understood that depending on the size of the virus, the virus titer, throughput and competition due to impurities the recovery of the virus may vary. However, for a particular virus the virus capacity of the bead and the virus recovery is governed by the external surface area per unit volume which in turn is determined by the size of the bead.

3.3. Purification of influenza virus

Virus purification technology should provide both high virus recovery and good impurity removal. To determine whether use of bigger beads could provide satisfactory impurity removal in addition to good virus recoveries, the flow-through purification of influenza virus type A/WS (H1N1 strain) was studied. For this study separate columns containing, 90 μm AEX beads (0.8 ml, Control), 200 μm AEX beads (0.8 ml, Prototype-1), 200 μm AEX-CEX beads (1.6 ml, Prototype-2), 200 μm AEX-HIC beads (1.6 ml, Prototype-3) and 200 μm AEX-CEX-HIC beads (2.4 ml, Prototype-4) were challenged with impure feed of influenza virus type A/WS (H1N1 strain), prepared as described in Section 2.2.3. AEX columns with additional CEX and HIC beads were also tested with the expectation that they would offer greater impurity clearance by capture of a wide variety of host cell proteins with different isoelectic points (p*I*) and hydrophobicity. Columns with more than one bead type contained equal proportions of the different beads packed one below the other in the sequence mentioned above. To determine whether layering the different beads as opposed to mixing them randomly had an effect on the results of the experiment an additional column containing 200 μm AEX-CEX-HIC beads (2.4 ml, Prototype-5) mixed randomly together was also tested. The column with 90 μm AEX beads served as the control for the experiment.

The impure influenza feed was processed through the columns at 0.16 ml/min which corresponds to a 5 min residence time per

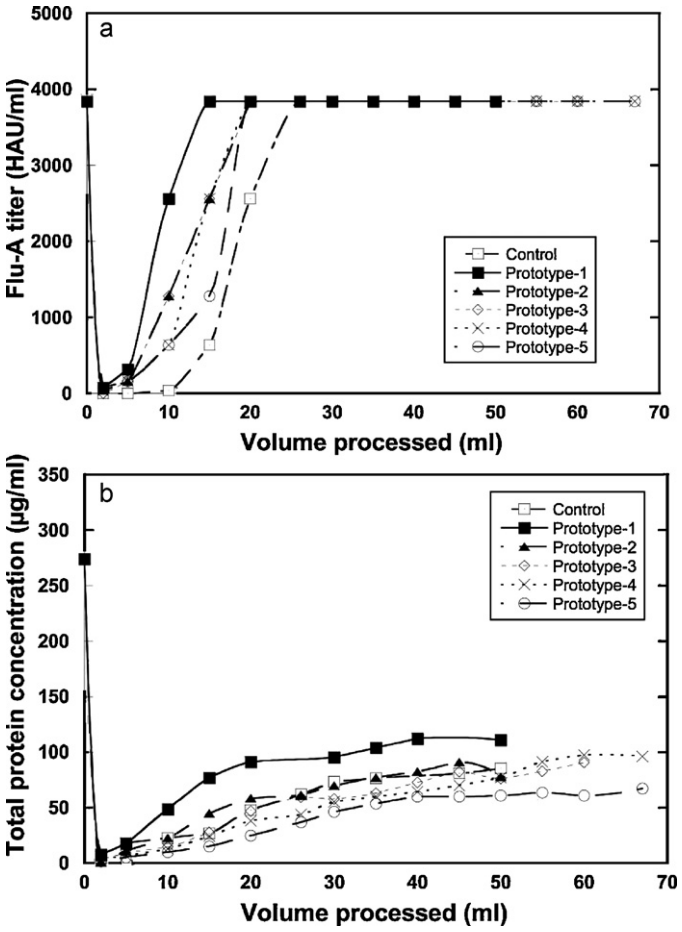

Fig. 6. Nature of the breakthrough of (a) influenza virus type-A (Flu A) and (b) total protein, processed in flow-through mode via [□] 90 μm AEX beads (0.8 ml, Control), [■] 200 μm AEX beads (0.8 ml, Prototype-1), [▲] 200 μm AEX-CEX beads (1.6 ml, Prototype-2), [◊] 200 μm AEX-HIC beads (1.6 ml, Prototype-3), [x] 200 μm AEX-CEX-HIC beads (2.4 ml, Prototype-4) and [○] 200 μm mixed AEX-CEX-HIC beads (2.4 ml, Prototype-5) columns from an impure feed stream containing the virus, HCP and HC-DNA in 50 mM Tris buffer at a fixed residence time of 5 min through the AEX beads in the column.

bead type in the column. To imitate typical throughputs in a chromatographic process a total of 50–67 ml of feed was processed through each column which corresponds to 28–62 CV depending on the size of the column used. The flow-through from the columns was collected in 1 ml fractions and assayed for concentration of virus, total protein and HC-DNA to determine the break-through curve for both virus and impurities. The area under the virus breakthrough curve was used to calculate the virus recovery whereas the area above the impurity break through curve was used to calculate the impurity clearance.

As expected, it can be seen in Fig. 6a that the virus breaks through the 200 μm bead columns earlier than the 90 μm beads which translates into the higher virus recoveries seen in Table 1. On the other hand the total protein breakthrough of the 90 and 200 μm AEX bead columns (Control and Prototype-1) are comparable, as seen in Fig. 6b. The protein removal by the 200 μm AEX beads is ~10% lower than the 90 μm AEX beads as seen in Table 1. This may be due to greater diffusion resistance encountered by the protein to access the internal surface area of the larger beads. However this is not a significant decrease and can be negated by minimal increase of residence time in the column or by using beads with larger pores. Further it can be noted that the addition of CEX and HIC beads to the columns reduces the total protein breakthrough and improves the total protein clearance. As seen in Table 1 the total protein clearance by Prototypes 3, 4 and 5 exceeds the clearance of the 90 μm bead column. This improvement however is most likely due to the removal of a different segment of the host cell proteins that do not bind to the AEX beads. In addition it may be noted that the improvement in impurity removal with addition of CEX and HIC beads is only 15–20% for this feed stream, suggesting that there may be only a small population of these proteins that can bind to the beads under these buffer conditions. Hence equal volumes of CEX and HIC beads may not be required to remove these impurities allowing use of a smaller column size. Also considering the fact that the buffer conditions used in this study was most conducive to only AEX beads, optimizing buffer conditions for the bead mixture may further help improve total protein clearance.

The volume at which influenza virus breaks through column Prototype-1 is approximately half that of the control column. This suggests that the 90 μm AEX bead column binds approximately two times the amount of virus as the 200 μm AEX bead column. This observation is in line with the theory that the capacity of the beads for molecules that bind only to their external surface area should change according to the ratio of their diameter and is responsible for the higher virus recovery from Prototype 1. The addition of CEX and HIC beads appears to slightly decrease the virus recovery, as seen for Prototypes 3–5. But this change is insignificant considering the fact that the product purity increases considerably over that of the 90 μm AEX bead column, as seen in Table 1. The minimal loss of virus suggests negligible interactions between the virus and the CEX and HIC beads. This may be because the overall negative charge of the virus at pH 8, at which the test was performed. Hence, for this application small sized CEX and HIC beads could potentially be used in combination with larger AEX beads. This would reduce residence times, minimize the volume of CEX and HIC beads required, reduce column size and help achieve better total protein clearance. Based on the results shown in Table 1 it can be concluded that a combination of AEX and HIC beads may provide optimum impurity removal while maintaining good virus recoveries.

The breakthrough curves of the HC-DNA follows a trend similar to that of the virus, as seen in Fig. 7. The volume at which DNA breaks through the 200 μm AEX beads is approximately 50% that of the 90 μm beads. This behavior of HC-DNA is due to their large size similar to that of influenza virus. The average size of HC-DNA is typically greater than the pores of the bead [31–33], thereby allowing binding only to the exterior of the beads. As a result the overall DNA clearance by Prototype-1 is lower than the control column as seen in Table 1. In addition use of CEX and HIC beads did not appear

Table 1
Total yield of influenza virus-type A (Flu-A), total protein clearance and total HC-DNA clearance from an impure feed stream in 50 mM Tris buffer calculated for a flow-through pool volume of 42 ml.

Type of column	% Flu-A recovery	% Total protein clearance	% DNA clearance	Impurity (ng protein/HAU)	% Improved recovery	% Improved purity
Control	57	82	82	22		
Prototype-1	80	72	62	24	29	
Prototype-2	72	81	54	18	21	18
Prototype-3	72	84	72	15	21	29
Prototype-4	71	86	62	14	20	36
Prototype-5	67	88	76	12	17.5	44

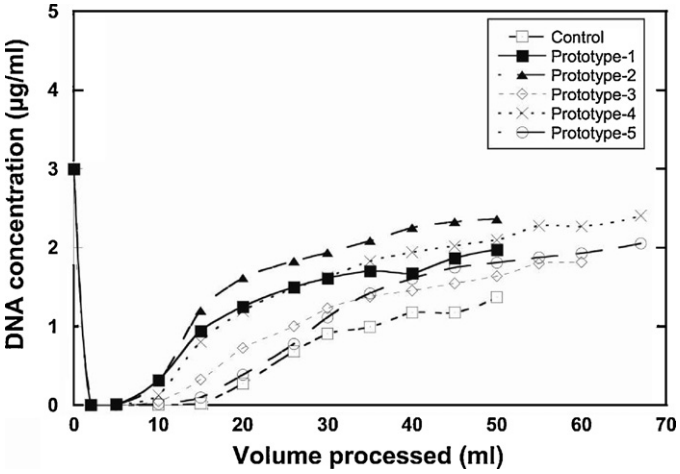

Fig. 7. Nature of the breakthrough of HC-DNA for the feed, columns and processing conditions described in Fig. 6.

to improve the DNA clearance very much as it is not expected to have significant interactions with these bead types.

A possible approach to improve the DNA removal would to treat the feed with nucleases such as Benzonase® (Merck KGaA) prior to chromatography, as is done in most industrial processes. Benzonase® breaks down single and double stranded DNA into smaller fragments of 2–5 bp in length [34]. These would then likely be removed by the flow-through process as their smaller size would allow them to diffuse into the pores and bind to the internal surface area of beads in a manner similar to host cell protein.

Purification of influenza virus using bind and elute anion exchange chromatography has been reported in the literature with varying degree of success. Banjac M. and coworkers [16] have demonstrated recovery of influenza virus of up to 35–50% (based on HA activity) with reasonable protein removal and good DNA removal using anion exchange monolith columns. On the other hand Kalbfuss et al. [14] have shown that average virus recoveries of up to 72% can be achieved using anion exchange membranes. However they only observed a moderate removal of host cell protein of c.a. 75% and no DNA removal. These studies illustrate that there is a trade off between virus recovery and impurity removal using anion exchange chromatography in bind and elute mode. Virus recoveries can also be dependent on the properties of the viral feed stream and the virus strain being purified. Hence to get a first hand account of the virus recovery from anion-exchange chromatography in bind and elute mode, the influenza virus bound to the 90 and 200 μm AEX beads (Control and Prototype-1) was eluted using a step gradient of 1 M NaCl. While step elution does not fractionate the virus from the impurities being eluted, it can effectively estimate the total virus recovery. The virus recoveries were ~45 and 38% for the 90 and 200 μm AEX beads respectively which is much lower than the yields obtained for the same resins in the flow-through mode. This result clearly demonstrates that flow-through separation using bigger beads has an advantage over bind and elute anion-exchange chromatography for purification of larger bio-molecules.

3.4. Optimization of virus recovery and impurity clearance for process development

In a flow-through process virus recovery and impurity clearance changes with the amount of feed that is processed through the column. The virus recovery at smaller column volumes is poor but improves as the amount of feed processed through the column increases. Conversely, impurity clearance is high at smaller column volumes and decreases with increase in throughput. Hence during process development of a flow-through chromatographic operation the throughput needs to be optimized to maximize yield and purity of the product. In this section a simplistic approach to perform such an optimization is suggested via the influenza virus purification process discussed above.

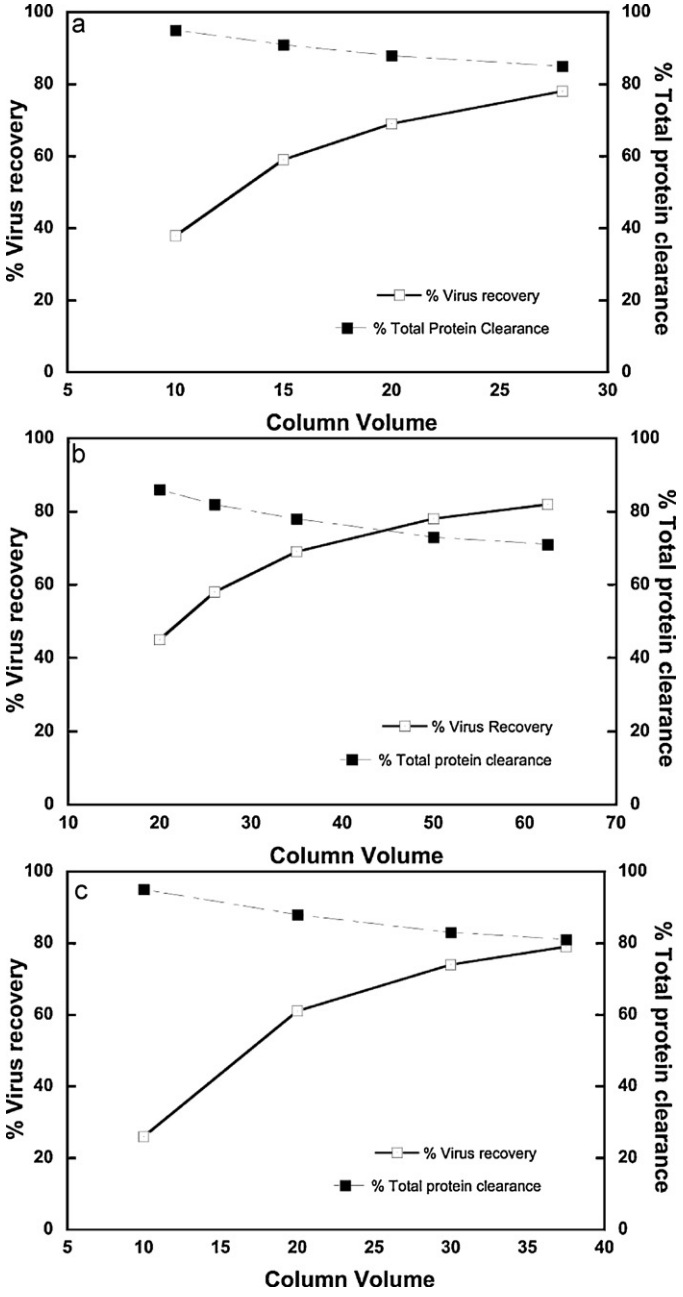

Fig. 8. Change in virus recovery and total protein clearance with feed throughput for (a) Prototype-1, (b) Prototype-3 and (c) Prototype-5.

The virus recovery at different volumes of feed processed through the column prototypes was calculated from the area under the curve in Fig. 6a. Similarly, the total protein clearance by these columns at the corresponding throughputs was calculated using the area above the break-through curve in Fig. 6b. While only the optimization of Prototype-1, Prototype-3 and Prototype-5 is discussed in this section, a similar procedure could be adopted for the remaining prototypes or any other application.

As seen in Fig. 8 and Table 2 the virus recovery increases and the impurity clearance decreases with throughput for all three

Table 2
Change in the virus recovery and total protein clearance with feed throughput for prototypes 1, 3 and 5.

Prototype-1			Prototype-3			Prototype-5		
CV	% Flu recovery	% Total protein clearance	CV	% Flu recovery	% Total protein clearance	CV	% Flu recovery	% Total protein clearance
20	45	86	10	26	95	10	38	95
26	58	82	20	61	88	15	59	91
35	69	78	30	74	83	20	69	88
50	78	73	37.5	79	81	27.9	78	85
62.5	82	71	38	80[a]	80[a]	32.5	83.3[a]	83.3[a]

[a] Extrapolated from graph in Figs. 6 and 8.

prototypes. The point at which the virus recovery and impurity clearance curves meet signifies the optimum number of CV of feed that can be processed through the column in flow through mode. At the optimum point of operation both the virus recovery and total protein clearance are maximized and corresponds to the most efficient mode of operating the column. Below this point the product obtained would have less impurity but virus recovery would be inefficient whereas beyond this point virus recoveries would be high but impurity removal would be inefficient. Hence operating at this point would lead to most efficient and economical chromatographic separation. During process development the entire recovery and impurity curves do not need to be determined. One can perform a small experiment to obtain the trends in the curves and then extrapolate them to obtain the tentative operating point as shown for Prototypes 3 and 5.

It can be noted that the optimum operating point for Prototypes 1, 3 and 5 increased from 75 to 83.3%, whereas the column volumes of feed that were processed through them decreased from 45 to 32.5 CV. The shift in the optimum point of operation is in the order of increase in the impurity clearance by these columns shown in Table 1. Higher impurity removal allowed larger volume of feed to be processed through these columns. Although the CV of feed processed through the columns decreased due to increase in the size of the columns from 0.8 to 2.4 ml, the overall volume of feed that was processed through the columns while maintaining high impurity clearance at the optimum operating point increased from 36 to 78 ml (extrapolated from Fig. 8c). Both these factors together lead to more efficient chromatographic operation using Protoype-5. While the higher efficiency of Prototype-5 comes at the cost of using additional beads (HIC and CEX) this cost is negated by the higher virus recovery, impurity removal, volume of feed processed and minimal post processing of product if required. The use of three different types of beads could be overcome by using mixed mode resins. Since impurity clearance appears to hold the key to improvement in efficiency, use of beads with higher capacity for impurities could potentially lead to both smaller columns and higher optimum operating conditions thereby lowering the resin cost.

4. Conclusions

The above study successfully demonstrates that virus can be efficiently purified in a flow-through mode. Use of big beads with optimized diameters is a good way to minimize external surface per unit volume in a column. This technique when optimized can allow high recovery of virus without causing diffusion limitations for impurity binding and hence does not compromise on impurity clearance or capacity. Virus recovery as high as 80% was achieved by increasing the bead size to 200 μm. Theory and experimental results suggest that beads with larger diameter would result in recovery of virus greater than 80%. In addition total protein clearance of up to 80–85% could be achieved using a combination of different beads. The total protein clearance can be further improved by using mixed mode or tailor made resins. On the other hand HC-DNA clearance of only about half a log was achieved suggesting that this technology does not provide adequate removal of whole DNA. However this issue can be easily addressed by pre-treating the feed with nucleases before processing it through the column so as to allow satisfactory removal of DNA. Process optimization for the flow-through virus purification process was straightforward and provided insight for further improving the technique. While proof of concept has been demonstrated in this article to reveal the potential of this technology, similar optimization of methods should be considered for specific applications to achieve process improvements. As this technique allows recovery of only unbound virions under mild processing conditions the risk of loss of infectivity of the virus being purified is low. Further, depending on the impurity load the technology can be either used for early stage downstream processing or final polishing step provided some virus loss is acceptable at this stage. Given the ability to separate any nano-particle, simple mode of operation, good performance, high throughput and scalability this approach has the potential to be a universal purification technique.

Acknowledgements

We thank Dr. Nanying Bian, Neil Soice and Dr. Priyabrata Pattnaik for their helpful comments and support.

References

[1] S.K. Powell, M.A. Kaloss, A. Pinkstaff, R. McKee, I. Burimski, M. Pensiero, E. Otto, W.P. Stemmer, N.W. Soong, Nat. Biotechnol. 18 (2000) 1279.
[2] M. McGrath, O. Witte, T. Pincus, I.L. Weissman, J. Virol. 25 (1978) 923.
[3] K. Saha, Y.C. Lin, P.K.Y. Wong, J. Virol. Methods 46 (1994) 349.
[4] K. Okuda, K. Itoh, K. Miyake, M. Morita, M. Ogonuki, S. Matsui, J. Clin. Microbiol. 1 (1975) 96.
[5] B. Sathananthan, E. Rødahl, T. Flatmark, N. Langeland, L. Haarr, APMIS 105 (1997) 238.
[6] A.A. Kumar, Y.U. Rao, A.L. Joseph, K.R. Mani, K. Swaminathan, J. Biosci. Bioeng. 94 (2002) 375.
[7] C.B. Reimer, R.S. Baker, R.M. vanFrank, T.E. Newlin, G.B. Cline, N.G. Anderson, J. Virol. 1 (1967) 1207.
[8] J. Vorlop, C. Frech, H. Lubben, J.P. Gregersen, Method for producing an active constituent of a pharmaceutical or a diagnostic agent in an MDCK cell suspension culture, US20050118140A1 (2005).
[9] T. Rodrigues, A. Carvalho, A. Roldão, M.J.T. Manuel, C. Carrondo, P.M. Alves, P.E. Cruz, J. Chromatogr. B 837 (2006) 59.
[10] L. Opitz, J. Salaklang, H. Buttner, U. Reichl, M.W. Wolff, Vaccine 25 (2007) 939.
[11] Anon, Heparin as pseudo affinity chromatography ligand in influenza virus purification, 2006 (IPCOM000140661D).
[12] J.O. Konz, R.C. Livingood, A.J. Bett, A.R. Goerke, M.E. Laska, S.L. Sagar, Hum. Gene Ther. 16 (2005) 1346.
[13] F. Blanche, A. Barbot, B. Cameron, Method for separating viral particles, US6537792B2 (2003).
[14] B. Kalbfuss, M. Wolff, L. Geisler, A. Tappe, R. Wickramasinghe, V. Thom, J. Udo Reichl, Membr. Sci. 299 (2007) 251.
[15] P. Kramberger, R.C. Honour, R.E. Herman, F. Smrekar, M. Peterka, J. Virol Methods 166 (2010) 60–64.
[16] M. Banjac, P. Kramberger, B. Lah, M. Jarc, A. Štrancar, E. Maurer, F. Gelhart, M. Gassner, H. Seper, T. Muster, M. Peterka, Poster www.biaseparations.com/library/includes/file.asp?FileId=251.
[17] M. Phillips, J. Cormier, J. Ferrence, C. Dowd, R. Kiss, H. Lutz, J. Carter, J. Chromatogr. A 1078 (2005) 74.
[18] U. Metha, Bioprocess Int. Industry Yearbook, 2009, p. 84.
[19] M. Jahanshahi, Z. Zhang, A. Lyddiatt, IEE Proc. Nanobiotechnol. 152 (2005) 121.
[20] P.E. Gustavsson, R. Lemmens, T. Nyhammar, P. Busson, P.O. Larsson, J. Chromatogr. A 1038 (2004) 131.

[21] E. Spakman, Avian Influenza Virus-Methods in Molecular Biology, 1st ed., Humana Press, Totowa, 2008.
[22] L. Opitz, S. Lehmann, U. Reichl, M.W. Wolff, Biotechnol. Bioeng. 15 (2009) 1144.
[23] S.P. Hansen, R. Faber, U. Reichl, M. Wolff, A.P. Gram, Purification of vaccinia viruses using hydrophobic interaction chromatography, US20100119552 A1 (2010).
[24] G. Oster, J. Biol. Chem. 190 (1951) 55.
[25] S. Olofsson, Arch. Virol. 49 (1975) 93.
[26] R. Hunt, Herpes Viruses, Biomedical Sciences Graduate Program, Web: February 14, 2011. Available from: <http://pathmicro.med.sc.edu/virol/herpes.htm>.
[27] K. Wallvik, Biochim. Biophys. Acta 322 (1973) 75.
[28] Sigma Aldrich Product Information, Albumin from bovine serum, Application Note-A2058.
[29] H. Brough, C. Antoniou, J. Carter, J. Jakubik, Y. Xu, H. Lutz, Biotechnol. Prog. 18 (2002) 782.
[30] P.V. Magnus, Bull. World Health. Org. 8 (1953) 647.
[31] B.E. Boyes, D.G. Walker, P.L. McGeer, Anal. Biochem. 170 (1988) 127.
[32] F. Devínsky, M. Pisárčik, I. Lacko, Gen. Physiol. Biophys. 28 (2009) 160.
[33] J.J. McFadden, P.D. Butcher, R.J. Chiodini, J. Hermon-Taylor, J. Gen. Microbiol. 133 (1987) 211.
[34] Benzonase® Nuclease, Novagen Technical Notes-TB261 02/00.